J. Physiol. (1985), **364**, *pp.* 359–379
With 1 *plate and* 11 *text-figures*
Printed in Great Britain

THE MECHANICAL PROPERTIES OF CILIARY BUNDLES OF TURTLE COCHLEAR HAIR CELLS

BY A. C. CRAWFORD AND R. FETTIPLACE
From the Physiological Laboratory, University of Cambridge, Cambridge CB2 3EG

(*Received 8 January 1985*)

SUMMARY

1. The mechanical behaviour of the ciliary bundles of hair cells in the turtle cochlea was examined by deflecting them with flexible glass fibres of known compliance during simultaneous intracellular recording of the cell's membrane potential.

2. Bundle motion was monitored through the attached fibre partially occluding a light beam incident on a photodiode array. The change in photocurrent was assumed to be proportional to bundle displacement.

3. For deflexions of 1–100 nm towards the kinocilium, the stiffness of the ciliary bundles was estimated as about 6×10^{-4} N/m, with the fibre attached to the top of the bundle.

4. When the fibre was placed at different positions up the bundle, the stiffness decreased approximately as the inverse square of the distance from the ciliary base. This suggests that the bundles rotate about an axis close to the apical pole of the cell and have a rotational stiffness of about 2×10^{-14} N . m/rad.

5. Step displacements of the fixed end of the flexible fibre caused the hair cell's membrane potential to execute damped oscillations; the frequency of the oscillations in different cells ranged from 20 to 320 Hz. Displacements towards the kinocilium always produced membrane depolarization.

6. The amplitude of the initial oscillation increased with displacements up to 100 nm and then saturated. For small displacements of a few nanometres, the hair cell's mechanoelectrical sensitivity was estimated as about 0·2 mV/nm.

7. Force steps delivered by the flexible fibre caused the bundle position to undergo damped oscillations in synchrony with the receptor potential. The mechanical oscillations could be abolished with large depolarizing currents that attenuated the receptor potential.

8. When placed against a bundle, a fibre's spontaneous motion increased and became quasi-sinusoidal with an amplitude several times that expected from the compliance of the system. It is suggested that the hair bundle drives the fibre.

9. We conclude that turtle cochlear hair cells contain an active force generating mechanism.

INTRODUCTION

Cochlear hair cells are thought to detect the relative motion of the basilar and tectorial membranes as a result of deformation of their stereociliary bundles. Near auditory threshold, the amplitude of vibrations of the basilar membrane have been estimated to be of the order of 0·3 nm (Rhode, 1978; Khanna & Leonard, 1982; Sellick, Patuzzi & Johnstone, 1982; Crawford & Fettiplace, 1983), although it is not clear that the hair cells themselves can respond to such small displacements without additional mechanical amplification. Direct manipulations of hair bundles in the frog saccule have been shown to generate a membrane conductance change leading to a receptor potential (Hudspeth & Corey, 1977), which was examined for calibrated bundle displacements of relatively large amplitude. The mechanism linking the mechanical stimulus to the transducer conductance is unknown.

The object of the work to be described is a quantitative analysis of the mechanical properties of the hair bundles. The approach has been to measure the bending of a single bundle in the turtle cochlea by attaching it to a flexible glass fibre, and monitoring the fibre's motion through its shadowing of a light beam falling on a photodiode array. The method allows displacements of 1–500 nm to be recorded and, with simultaneous recording of the receptor potentials, it has been possible to determine the range of forces and displacements to which the cells can respond. The technique is also suitable for measuring any active forces generated by individual hair cells, which have been proposed on theoretical grounds as a means of boosting the basilar membrane vibrations at sound levels near threshold (Kemp, 1979; Kim, Neely, Molnar & Matthews, 1980; Mountain, Hubbard & McMullen, 1983; Bialek, 1983).

METHODS

Preparation

Experiments were performed on the isolated cochlear duct of the turtle *Pseudemys scripta elegans*. Animals were decapitated, the head bisected in the sagittal plane and the brain removed. After opening the cranial aspect of the otic capsule the entire membranous labyrinth, with the exception of the semicircular canals, was removed and immersed in artificial perilymph (composition in mM: NaCl, 130; KCl, 4; $CaCl_2$, 2·8; $MgCl_2$, 2·2; glucose, 4: HEPES, 5, pH 7·6). The reunient duct was cut, the vestibular apparatus discarded, and the vestibular membrane removed to expose the scala media. The roof of the scala tympani was then cut away together with the nerve to the posterior semicircular canal, leaving a preparation consisting only of the cochlear partition and its surrounding ring of limbic tissue. Before removing the tectorial membrane the preparation was digested for 15 min in perilymph containing subtilisin BPN′ (Sigma) 30 μg/ml at room temperature. This digestion served to ease removal of the tectorial membrane and partially to dissolve the subtectorial material (Miller, 1978) immediately surrounding the ciliary bundles. The preparation was then secured in the experimental chamber with tungsten pins, washed free of enzyme, and mounted on the stage of a limb-focusing compound microscope.

The microscope consisted of a stand, Carl Zeiss (Jena), Ergeval, modified to take Carl Zeiss (Oberkochen) optics throughout and was equipped either for Nomarski differential interference microscopy or bright field. The primary image formed by the water-immersion objective (×40 achromat N.A. 0·75) could be viewed with oculars using Nomarski optics, or projected onto a screen and photodiode array for photometry. In the latter case both polarizer and analyser were removed from the beam. The light source (Zeiss 100 lamphouse with 12 V 100 W tungsten–halogen lamp) was run with a constant direct current of 8·2 A with a heat filter in the light path. The microscope and photometric apparatus were mounted on an antivibration table. All experiments were carried out at room temperature (21–25 °C).

Mechanical stimulation

Single ciliary bundles were displaced along the preferred axis of the cell (the plane orthogonal to the long axis of the basilar membrane and bisecting the kinocilium; Shotwell, Jacobs & Hudspeth, 1981), using a fine glass fibre of known compliance. The fibre was glued to a glass stub mounted on a piezoelectric driver constructed from a short length of Vernitron bimorph (type PZT-5B) operating in the cantilever mode. The length of the piezoelectric element was 8 mm and the length of the glass stub about 15 mm. Details of the construction of similar cantilever drivers are given in Corey & Hudspeth (1980). The electromechanical sensitivity of the driver was 0·125 μm/V and its lowest frequency of resonance 4·1 kHz. Voltage steps in the range $\pm$20 V were delivered to the bimorph via a six-pole low-pass Bessel filter the corner frequency of which was adjusted to about 1 kHz so as just not to excite the bimorph resonances. The 10–90 % rise time of the mechanical step was 0·4 ms. An example of the step response of the stimulator is given in Fig. 2.

Construction and calibration of fibres

Fibres were pulled by hand from 100 μm diameter soda glass rod. Segments about 0·5–1 μm diameter and 100–300 μm long were glued to a glass stub bolted to the piezoelectric element and after initial calibration (see below) trimmed to a length expected to give a final stiffness of about 10^{-4} N/m, using the assumption that fibres obeyed the equation for a perfect cantilevered beam. All fibres were then recalibrated. Clean, freshly prepared fibres stuck tightly to the ciliary bundles to the extent that a bundle was visibly damaged if an attempt was made to pull the fibre away. This strong adhesion rarely persisted after contact with more than a few bundles and for this reason a new fibre was usually used for each experiment.

Calibration of the stiffness of glass fibres followed, in essence, the method of Yoneda (1960). A standard fibre drawn from quartz 940 μm long and 2·5 μm in diameter was calibrated by hanging small crystals of *p*-nitrophenol (Sigma spectrophotometric grade) at its tip and measuring, with a horizontal compound microscope fitted with a screw micrometer eyepiece, the deflexion that these small weights produced. The masses of the crystals (0·15–7·5 μg) were then determined spectroscopically, using the procedure given in Lowry & Passonneau (1972). The standard fibre obeyed Hooke's law over the range of deflexions used (3–110 μm) and had a stiffness of $6{\cdot}8 \times 10^{-4}$ N/m. This standard fibre was then used to deflect the tips of other fibres of greater but unknown compliance, so as to obtain the ratio of the compliances. The errors involved in this reciprocity method are discussed by Yoneda (1960).

Since the quartz fibre was uniform, its stiffness, K_Q, could also be deduced from the equation for a cantilever beam (Case & Chilver, 1971):

$$K_Q = \frac{3\pi E r^4}{4l^3}, \tag{1}$$

where r is the radius, l the length and E Young's modulus which for quartz is $7{\cdot}3 \times 10^{10}$ N/m^2 (Kaye & Laby, 1975). The value of K_Q calculated was $5{\cdot}1 \times 10^{-4}$ N/m, agreeing well with the measured stiffness.

Detection of the movements of the fibre tip

If the tip of a calibrated fibre is placed against a ciliary bundle and the other end moved through a known distance using the piezoelectric element, the stiffness of the bundle can be measured if the deflexion of the end in contact with the bundle is known (see Results). This method was first employed by Yoneda (1960) and subsequently by Strelioff & Flock (1984) using displacements large enough to be visualized. Stiffness measurements below the limits of visual resolution (the range in these experiments involved bundle displacements of 1–500 nm) require an optical movement detector. The scheme employed is illustrated in Fig 1. With the preparation illuminated in bright field the secondary image of the microscope was formed on a screen by a 20 $\times$ ocular used as a projective lens. The distance from screen to ocular was adjusted so that the image of the fibre was about 0·5 mm in width and thus filled about half the field of a double photodiode array (2 mm $\times$ 0·5 mm; Centronics LD 2–5) mounted at the centre of the screen. Provided that the excursions of the image do not exceed the borders of the photodiode array, the difference in the photocurrents between the two diodes should be proportional to the displacement of the image. This proportionality was verified for steady displacements of the fibre in free solution of 1–500 nm.

The photodiodes, mounted on an $X-Y$ micrometer from an optical bench, could be centred on the fibre image by adjusting their position until the difference in photocurrents was zero. The absolute displacement could be determined by moving one end of the fibre through a known distance with the piezoelectric element and following the change in photocurrent as the other end, when not on the ciliary bundle, moved through the same distance. An example of this procedure is illustrated in Fig. 2 which also shows the movement of the tip of the fibre when placed against a ciliary bundle.

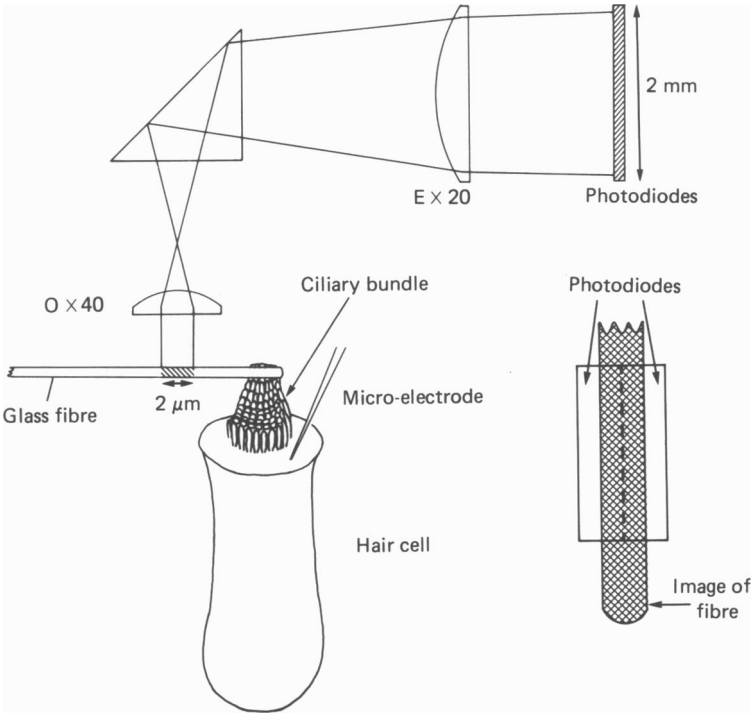

Fig. 1. Schematic arrangement of the apparatus for measuring motion of a hair cell stereociliary bundle. The basilar papilla was placed on the fixed stage of a compound microscope with the bundles facing upwards; only a single hair cell is illustrated. One end of a flexible glass fibre (typical dimensions: length 100 μm, diameter 0·5 μm) was attached to the tallest row of cilia, and the other end was fixed to a piezoelectric element, not shown. A 2 μm section of the fibre close to the point of contact with the bundle was imaged through an insulated water-immersion objective (O) (× 40 Zeiss Achromat) and × 20 eyepiece (E) (Zeiss KPL) onto a distant pair of photodiodes with a total magnification of about 1000. For hair cell stimulation, the fibre was driven towards the longest cilia, and the displacement deduced from the change in photocurrent; receptor potential was measured with an intracellular micropipette. Microscope optics not drawn to scale. 2 μm calibration bar on fibre also applies to hair cell. Inset: front view of pair of photodiodes with the image of the flexible fibre superimposed. Fibre magnified so that its image diameter is equal to width of one of the photodiodes (0·5 mm).

The band width of the detector system was limited to 1 kHz. Photon noise set the equivalent displacement noise floor at less than 1 nm r.m.s., sufficiently low to measure the Brownian motion of the fibres. When in contact with a ciliary bundle the fibres executed a quasi-sinusoidal motion, probably driven by the hair cell, and again well above the detection limits set by the photon noise.

Intracellular recording

Glass micropipettes (resistances 200–500 MΩ) were filled with 4 M-potassium acetate + 0·1 M-potassium chloride, and inserted into the apical surface of a hair cell at the border distant from the kinocilium. Electrodes were bent through a right angle about 500 μm back from the tip using the method of Hudspeth & Corey (1977). Since the depth of immersion of the pipettes could not be reduced to less than about 4 mm, the band width of the recording system even with capacity compensation, usually extended only to a few hundred hertz. To obtain a better frequency response the band width of the compensating amplifier was reduced to around 40 kHz. The value of this procedure (which places two poles in the feed-back loop) when using deeply immersed micropipettes, is discussed by Guld (1974). In our case it increased the band width of the recording system, as assessed by the rise time of the voltage drop across the electrode impedance during the flow of a known current step, to a few kilohertz.

The experimental procedure was first to obtain an intracellular recording from a hair cell, and then to place the end of a vibrating fibre onto the top of the hair bundle, usually on the surface facing the neural limb. The static position of the fibre and bundle was adjusted to produce the largest receptor potential in response to a step perturbation of the bundle, a few tens of nanometres in amplitude. This procedure for setting the resting position of the bundle was necessary because the hair cells did not show pronounced adaptation to changes in static position (as has been described by Corey & Hudspeth (1983) in the frog's sacculus) at least over a time period of tens of seconds. The adjustment was less than 200 nm. All data were stored on an FM tape recorder (band width 0–2·5 kHz) for subsequent analysis on a PDP11/34 laboratory computer.

RESULTS

Hair bundle stiffness

The mechanically sensitive component of each turtle hair cell consists of a bundle of about 100 stiff interconnected hairs or stereocilia that project from the cell's apical surface. Rows of hairs are graded in height across the bundle, and the tallest, attached to a single kinocilium, attains a height of 6–7 μm. The bundles are therefore morphologically polarized and, in the turtle cochlea, all have a common orientation with the kinocilium placed on the abneural side of the bundle (Miller, 1978). In the intact cochlear duct, these bundles are shrouded in pockets of the tectorial membrane, thought to be attached to the kinocilial bulb and tallest stereocilia (Miller, 1978). In the following experiments, designed to measure the mechanical properties of the bundles, the tectorial membrane was removed, and forces were delivered to a bundle directly by means of a flexible glass fibre in contact with the tallest cilia (see Fig. 1 and Pl. 1).

Fig. 2 shows average photovoltages representing motion of a flexible fibre on and off a hair bundle. When situated above the bundle the tip of the fibre reached a maintained displacement with a time constant of 2 ms; the steady displacement was assumed to be equal to the step imposed by the piezoelectric element, here 250 nm. With the fibre placed against the bundle, the over-all motion to the same step was much reduced, indicating that the hair bundle was about an order of magnitude stiffer than the fibre. The time course of the motion, which now became oscillatory, will be examined later in the paper.

Knowing the stiffness, K_f, of the fibre, and the displacement, y_2, of the end attached to the piezoelectric element, the force, F, required to deflect the bundle by a given amount, y_1, can be evaluated:

$$F = K_f(y_2 - y_1). \tag{2}$$

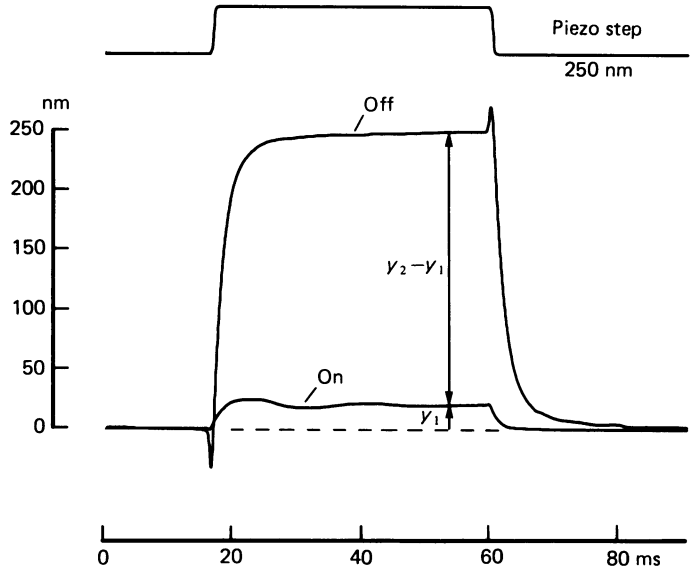

Fig. 2. Average photocurrents for displacements of a flexible fibre when placed at the tip of a ciliary bundle (on) or just above the same bundle (off). Top trace shows the time course of the voltage step delivered to the piezoelectric device. The ordinate calibration (in nanometres) was obtained by assuming that the steady deflexion of the free end of the fibre when not on the bundle was equal to that of the fixed end. Transients at beginning and end of step are thought to be due to a higher mode of vibration of the fibre which behaves like a cantilevered beam. The force delivered by the fibre can be calculated from its known stiffness (K_f, here 0·067 pN/nm) and the difference in steady displacements (y_1) on and (y_2) off the bundle; the bundle stiffness, K_B, is given by $K_B = K_f(y_2-y_1)/y_1$. About 300 records were averaged to produce each trace.

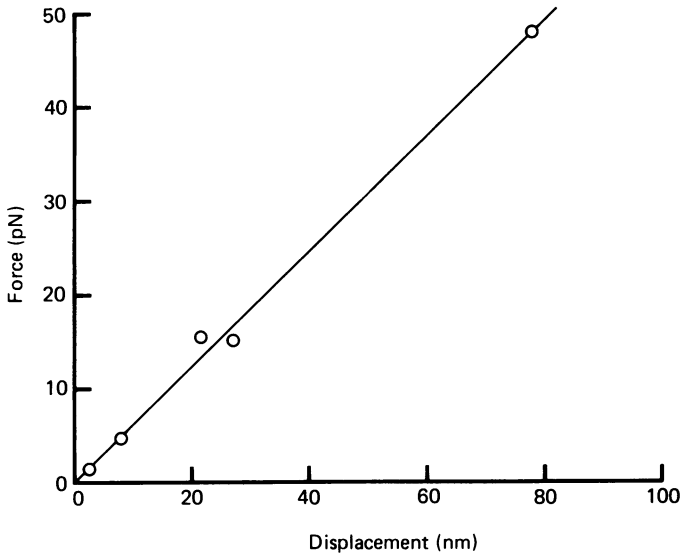

Fig. 3. Plot of force *versus* displacement of the ciliary bundle of a single hair cell made from average records similar to those in Fig. 2. Fibre was attached to the tip of the bundle and moved towards the kinocilium; measurements taken in steady state, about 40 ms after onset of step. Line drawn by eye through points gives a bundle stiffness of 0·62 pN/nm.

Force measurements are plotted in Fig. 3 for bundle deflexions of 2–80 nm, largely encompassing the operating range of the hair cell. Within this range, the force was proportional to steady displacement, implying that the bundle mounting behaved like a simple spring with a stiffness of 0·62 pN/nm ($6{\cdot}2 \times 10^{-4}$ N/m). Measurements on other cells, all made during simultaneous intracellular recording of the receptor potential, fell between 0·2 and 1·0 pN/nm (mean $\pm$ S.D. = $0{\cdot}59 \pm 0{\cdot}25$ pN/nm; $n = 15$). In these experiments, the fibre was attached to the top of the bundle and driven towards the kinocilium, a stimulus polarity regarded as being excitatory because it causes a depolarization of the hair cell membrane potential (Hudspeth & Corey, 1977; see also Fig. 6).

Under conditions where the fibre adhered strongly to a bundle, it was possible to compare stiffness values for motion towards and away from the kinocilium. This comparison was performed in three cells, and did not reveal any major asymmetry in the steady-state stiffness, an observation which differs from that of Strelioff & Flock (1984). In the three experiments, the mean ratio of stiffnesses for motion towards and away from the kinocilium was 0·91.

Mode of bending

For large displacements that can be directly visualized, the hair bundle appears to move as a rigid lever pivoted about its insertion into the apical pole of the cell (Flock, Flock & Murray, 1977). This hypothesis of bundle motion can be tested by measuring the apparent stiffness with the flexible fibre placed at different heights up the side of the bundle. The heights relative to the top surface of the cell, were determined to an accuracy of about 0·2 μm from the calibrated vertical micrometer scale on the Huxley manipulator to which the stimulating assembly was attached. The top surface of the cell was defined as the point at which the hexagonal array of ciliary rootlets was in focus. Measurements on six hair cells are given in Fig. 4 where the reciprocal of stiffness (compliance) is plotted in each case for three different fibre positions.

If the bundle behaves as though it were a rigid rod attached to a spring near the apical pole, then the torque around the base of the ciliary bundle may be expressed in terms of a rotational stiffness, K_R:

$$F\,h = K_R\,\theta, \tag{3}$$

where F is the force applied at a height h above the base, and θ is the angular deflexion of the bundle. For small θ, the measured stiffness K, defined as the force required to produce unit displacement at height h, is given by:

$$K(h) = \frac{K_R}{h^2}. \tag{4}$$

The continuous curve in Fig. 4, which is a reasonable fit to the points was calculated from eqn. (4) with a value of K_R of $1{\cdot}9 \times 10^{-14}$ N.m/rad. When plotted on double logarithmic coordinates, each set of measurements could be fitted with a straight line, the slope of which ranged from 1·3 to 2·1 (mean = 1·7). A relationship in which the compliance increases with the square of the height of the fibre up the bundle thus seems the most appropriate to describe the results.

The measurements are inconsistent with the view that the bundle can be treated as a cantilever beam, that is clamped at its base and moves by bending. From the treatment of a flexible beam (eqn. (1)) this hypothesis would predict that the compliance be proportional to the cube of the distance from the fixation point. A knowledge of the type of motion which the bundle undergoes may be important in

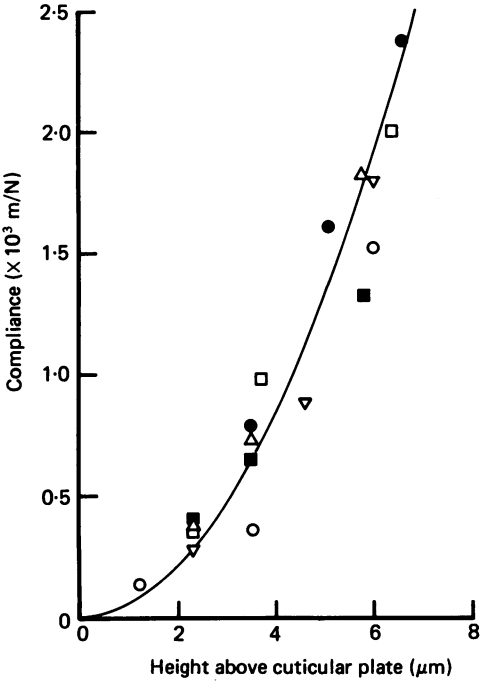

Fig. 4. Bundle compliance for six hair cells as a function of the vertical position of the fibre, which was placed on the abneural side of the bundle and driven away from the kinocilium. Ordinate is the reciprocal of stiffness obtained from force–displacement plots as in Fig. 3. Abscissa is the height of the fibre above the apical surface of the cell. Each symbol denotes a different cell. Smooth curve calculated from eqn. (4).

identifying the measured stiffness with a particular structural component of the hair cell.

Response–displacement curves

The main function of hair cells is to transduce mechanical vibrations, transmitted to the hair bundle, into changes in membrane potential. This section provides an estimate of the sensitivity of the transduction process. Fig. 5*A* shows hair cell receptor potentials evoked by calibrated bundle displacements towards the kinocilium, increasing in amplitude roughly by factors of three. These caused graded depolarizations of the membrane potential, which also exhibited damped oscillations during the bundle deflexion. The oscillations reflect the hair cell's frequency selectivity which differed from cell to cell (Fig. 6). Displacement–response plots obtained from measurements of such receptor potentials, are given for two cells in Fig. 5*B*. The peak depolarization occurring on the first cycle of the oscillation is plotted against the

bundle displacement, measured at the same point in time; the circles refer to the cell from Fig. 5*B* and the squares to another cell with similar sensitivity. In both cases, the receptor potential increased initially in proportion to displacement, but then saturated for displacements greater than 80 nm. These cells could therefore signal bundle position only for deflexions less than about 0·1 μm.

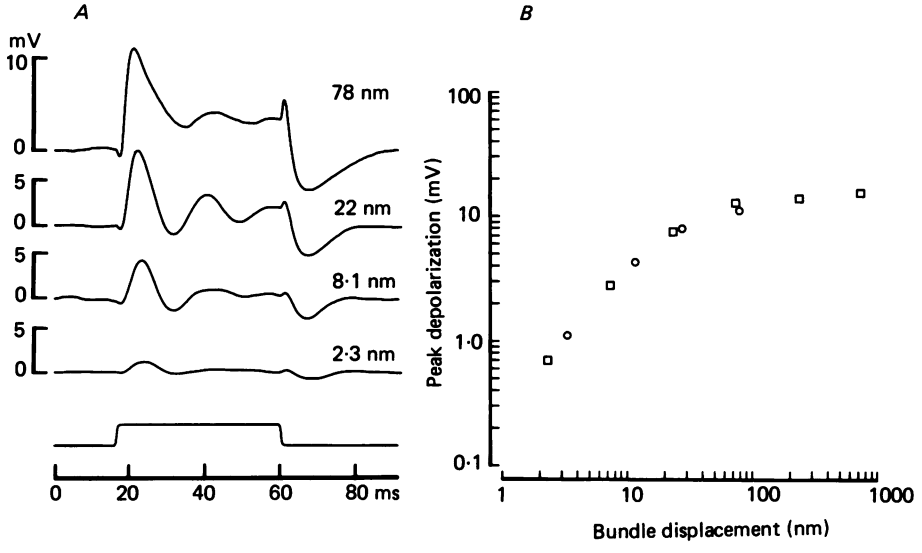

Fig. 5. *A*, receptor potentials for force steps delivered to the ciliary bundle by a flexible fibre; the steady displacements towards the kinocilium achieved are given beside traces, which are averages of 86–550 presentations. Time course of driving voltage to piezoelectric element is shown below and ordinates are membrane potentials relative to the resting potential (−47 mV). The flexible fibre had a stiffness about one-tenth of that of the bundle; same cell as Figs. 2 and 3. *B*, response–displacement plots for cell of *A* and one other. Ordinate is depolarization (relative to the resting potential) at the peak of the first cycle of the response. Abscissa, ciliary displacement towards the kinocilium measured at same point in time as receptor potential.

From the low level responses, the linear mechanoelectrical sensitivity of the transduction process could be estimated. For the cells illustrated, a value of 0·35 mV/nm was obtained and for other cells the sensitivity measured in this way normally exceeded 0·1 mV/nm (mean $\pm$ S.D. = 0·192 $\pm$ 0·097 mV/nm; n = 12).

Frequency selectivity

When steps are delivered with a fibre much more compliant than the bundle, the stimulus is approximately a force step and contains all frequencies. The evoked receptor potential contains information about the frequency selectivity of the transduction process, and has a form like that of a resonance (Crawford & Fettiplace, 1981*a*). Fig. 6 illustrates receptor potentials from four different cells: for each, the step response consisted of a damped oscillation at the onset and termination of the step, and the resonant frequency, given beside the traces, was different between cells. The results suggest that individual hair cells retain much of their frequency

selectivity in this isolated papillar preparation. Resonant frequencies from 20 to 320 Hz were observed in these experiments. They cover part of the range of resonant frequencies seen in the intact cochlea using sound stimulation, although there was a notable absence of higher frequency cells, which normally extend up to about 600 Hz. The reason for this discrepancy is unknown, although cells in the most basal region of the papilla, devoted to the higher frequencies (Crawford & Fettiplace, 1980), were rarely examined in the present experiments. The resonant frequency of a hair

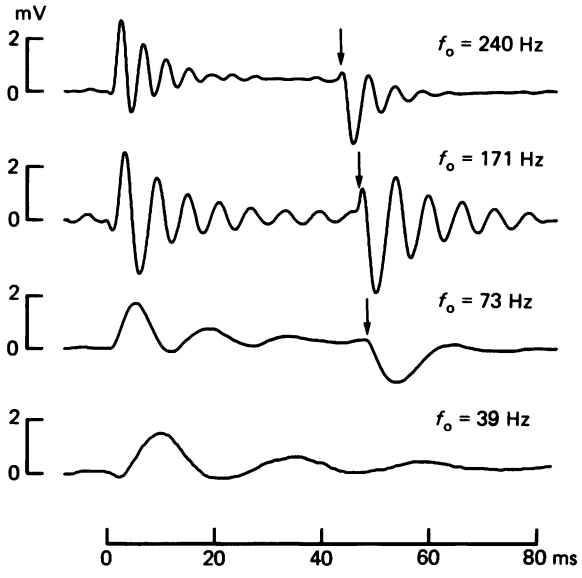

Fig. 6. Average receptor potentials for small displacements of ciliary bundle towards kinocilium in four hair cells tuned to different frequencies. For each example, the stimulus was delivered with a fibre more compliant than the bundle, began at time zero and ended at a time indicated by arrow; termination of response not shown for bottom record; steady bundle displacements from top to bottom: 30, 29, 7 and 10 nm. Note that receptor potentials consist of damped oscillations at start and end of deflexion, frequency of oscillations (f_0) given beside each trace. Ordinates are membrane potentials relative to resting potentials which from top to bottom were: −45, −49, −48 and −50 mV.

cell changed systematically with its position in the papilla; frequencies increased approximately exponentially from the lagenar to the stapedial end, an e-fold change in frequency occupying about 0·25 mm. The mean length of the papilla in ten preparations was 0·83 mm. Similar observations have been made previously on hair cells from the isolated ear in this animal (Crawford & Fettiplace, 1980) where the space constant was found to be about 0·14 mm. Thus the tonotopic organization of the papilla does not seem to be greatly disturbed by opening the cochlear duct or removing the tectorial membrane.

Damped oscillations in membrane potential could also be elicited by injection of extrinsic current steps through the recording electrode, as previously reported for the intact turtle cochlea (Crawford & Fettiplace, 1981*a*). In a given cell, the resonant frequency and quality factor (Q) of the tuning derived from the current-induced

oscillations were comparable to the values measured from similar responses to imposed hair bundle deflexions. A comparison of the responses to the two types of stimuli is illustrated in Fig. 7 for a cell with a resonant frequency of about 185 Hz and a Q of 5.

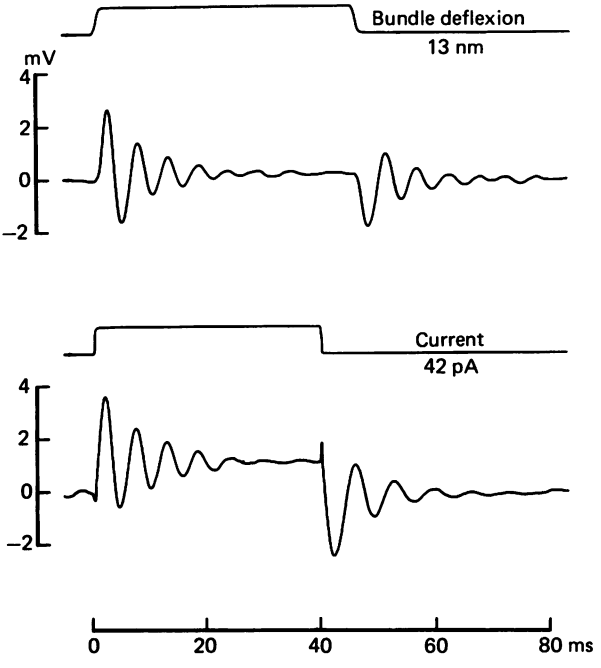

Fig. 7. Comparison of the average responses of a hair cell to small (13 nm) deflexions of the ciliary bundle (top) and injection of rectangular depolarizing currents (42 pA) through the intracellular electrode. Ordinates are membrane potential relative to resting potential (−46 mV). Number of responses averaged were 323 for the mechanical step and 149 for the current. From the oscillations at the onset of the responses, the resonant frequency and quality factor of tuning were 188 Hz and 4·7 (mechanical stimulus) and 181 Hz and 5·4 (current).

Bundle motion during force steps

Fig. 8 compares the time course of the receptor potential and bundle motion during a small step imposed by a flexible fibre. Throughout the stimulus the receptor potential underwent the usual damped oscillations, but surprisingly, those oscillations were also manifested in the bundle displacement. The amplitude of these mechanical oscillations was graded with the strength of the applied force, and, as a fraction of the change in steady level, was greatest for small deflexions of the bundle. The amplitude of the mechanical oscillations never exceeded 20 nm (peak-to-peak) even with much larger maintained displacements, and was always equal to or less than the steady displacement. As can be seen in Fig. 8 the form of the bundle displacement was not a replica of the membrane potential change, but its time course consisted of a scaled version of the membrane potential change superimposed upon a displacement pedestal.

Damped mechanical oscillations at the same frequency as those in the receptor

potential were seen in experiments on ten hair cells with resonant frequencies from 31 to 171 Hz. The mechanical oscillations were most prominent in cells with resonant frequencies below 100 Hz, and they were difficult to observe in higher frequency cells, which may be partly due to their attenuation as a result of viscous loading of the bundle by the fibre.

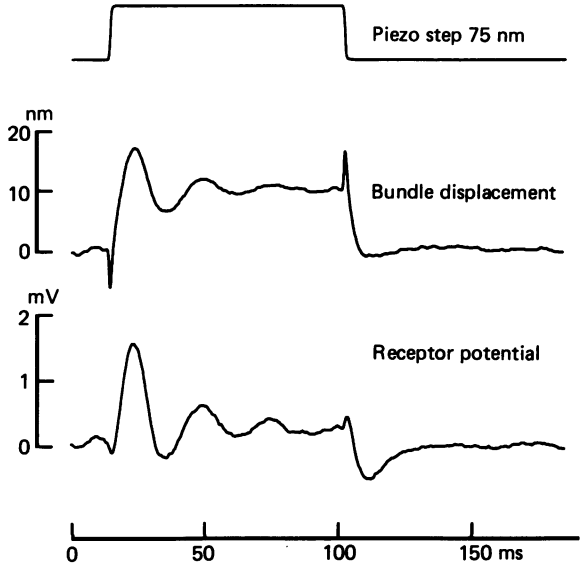

Fig. 8. Comparison of the time course of ciliary bundle displacement (middle trace) and receptor potential (bottom trace) when bundle forced towards the kinocilium with a flexible fibre attached to its tip. Driving voltage to piezoelectric element shown at top. For voltage reeord, ordinate is membrane potential relative to resting potential (−50 mV). Sixty-eight responses have been averaged to produce traces. Frequency of damped oscillations 39 Hz.

When placed upon the bundle, the fibre adds mass, stiffness, and viscous damping. Since the fibres have been constructed to have a stiffness much less than that of the bundle, the compliant element can be neglected. The other two types of load are, however, significant and affect not only whether the fibre disturbs the motion of the bundle, but also the accuracy with which bundle motion can be measured. Since the length of the fibre (100 μm) is very much longer than the length of the bundle (6 μm) the viscous damping on the fibre is likely to dominate the system. Viscous damping can be estimated from the time constant of motion of the fibre in free solution and its known compliance. Its value was about 4×10^{-7} N . s/m. The masses of fibre and bundle are comparable and of the order of 10^{-13} kg. These values, together with the stiffness of the bundle, indicate that the whole system will be heavily damped and have a time constant of about 1 ms. Forces applied to the system either via the fibre or by the hair cell should therefore lead to a progressively attenuated displacement at frequencies above about 150 Hz.

The fast initial and terminal transients visible in Fig. 8 are thought to be a consequence of higher modes of vibration of the flexible fibre, which for abrupt changes in position executed an initial 'back-flip' rather like a fishing rod. However,

the slower oscillations are unrelated to any resonances in the stimulating system, the lowest vibrational frequency of which was 4 kHz. When not attached to the bundle, the fibre gave no hint of oscillation, and although the back-flip was still evident, the subsequent motion was heavily over-damped (see Fig. 2). Furthermore, a given fibre could be used to measure mechanical oscillations in hair cells of quite disparate resonant frequencies, indicating that it was not the cause of the resonant behaviour.

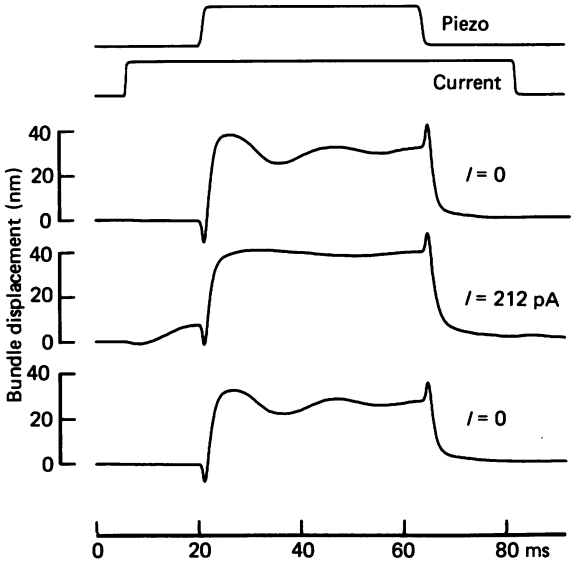

Fig. 9. Effects of current injection on mechanical oscillations. Each of lower three traces are average ciliary bundle displacements when forced towards the kinocilium with a flexible fibre. During the middle trace, there was an additional current pulse that depolarized the cell 33 mV from its resting potential (−45 mV). Timing of current pulse and voltage step to piezoelectric element shown above. Note that at the onset of the current there was a small displacement that had reached a steady level before the imposed deflexion of bundle occurred. 314–487 presentations averaged to produce traces.

Interaction of current injection and mechanical stimuli

The oscillations that have been observed in the bundle displacement are most likely an intrinsic property of the hair cells rather than a product of the measuring system. This view is supported by the demonstration that the amplitude of the oscillations could be altered by changes in hair cell membrane potential. Fig. 9 shows average displacement records before, during and after injection of large current pulses which depolarized the cell by 33 mV from its resting potential (−45 mV). The depolarization diminished the receptor potential, presumably by reducing the driving force for the flow of transducer current, which has a reversal potential around 0 mV (Crawford & Fettiplace, 1981*b*). It also reversibly abolished the oscillations in the bundle displacement, as would be expected if they were somehow linked to the receptor potential. Although not shown in the Figure, comparable hyperpolarizing currents also altered the form of the mechanical oscillations, quickening them and reducing their amplitude. Similar results with both depolarizing and hyperpolarizing currents were obtained from three other cells.

An additional effect visible in Fig. 9 is the small movement to the current pulse, the onset of which preceded the imposed mechanical step. In other experiments we looked for movements of the fibre, placed against the bundle, when extrinsic currents alone were injected across the hair cell membrane. When the current strength was

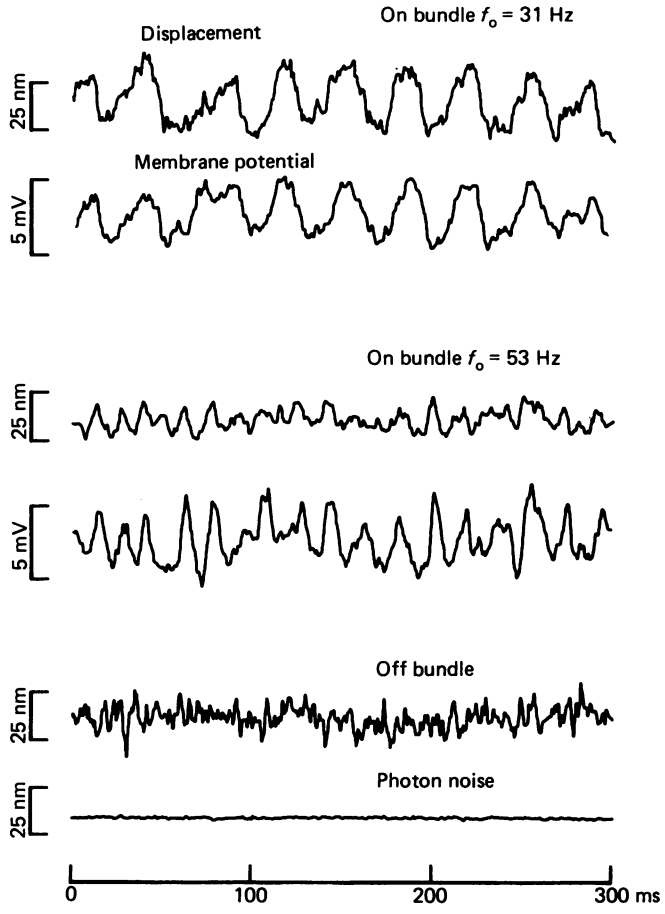

Fig. 10. Spontaneous mechanical and electrical activity in two hair cells. The top two pairs of traces are single sweeps of simultaneously recorded bundle displacement and membrane potential, and the displacement signals were obtained from motion of a flexible fibre attached to the ciliary bundle. The same fibre was used in both experiments and a sample of its spontaneous motion when not on the bundle is shown below; this is accompanied by an example of the photon noise expressed as an equivalent displacement, with the fibre not in the light beam. Resonant frequencies of cells given beside appropriate traces; stiffness of fibre 0·19 pN/nm. R.m.s. displacements were 11·2 nm (31 Hz cell), 6·0 nm (53 Hz cell) and 5·7 nm (off bundle).

kept below 100 pA so as to be within the range of currents capable of being generated by the mechanoelectrical transduction mechanism (Corey & Hudspeth, 1979; Crawford & Fettiplace, 1981*b*), displacements of the fibre up to ten nanometres were observed. Although small, the displacements evoked by current steps assumed the same oscillatory form as the membrane potential.

Spontaneous movements of the ciliary bundles

When the fibre was placed clear of the bundle the Brownian motion of its tip could be measured. In Fig. 10 an example of the photon noise in the detection system is given (expressed as an equivalent displacement noise) together with the motion of the fibre tip. The r.m.s. displacement of the fibre is about 6 nm which is close to the value expected from the fibre's stiffness. This is given by (Landau & Lifshitz, 1969; Bialek, 1983):

$$x_{\text{r.m.s.}} = (k_b T/K)^{\frac{1}{2}}, \quad (5)$$

where k_b is Boltzmann's constant, T the absolute temperature, K the stiffness and $x_{\text{r.m.s.}}$ the root mean square displacement. The expected value for $x_{\text{r.m.s.}}$ is 5 nm. When the fibre was placed against a bundle we expected the displacement to become smaller since the stiffness of the bundle–fibre combination is much greater than that of the fibre alone. In fact the opposite happened: when in contact with the bundle, the fibre underwent a larger r.m.s. displacement the spectral components of which were always limited to a narrow band of frequencies. For example, the r.m.s. displacement for the cell with a resonant frequency of 53 Hz, illustrated in Fig. 10, was 6 nm with the fibre on the bundle, whereas the r.m.s. displacement predicted solely on the basis of the stiffness of the ciliary bundle (0·77 pN/nm) should have been 2·3 nm. There seems little doubt that the bundle is actively driving the tip of the fibre under these circumstances.

It seems unlikely that the oscillations arise from general vibrations or instabilities of the preparation; large quasi-sinusoidal motion was not seen if the fibre was placed against the surface of the reticular lamina rather than against a ciliary bundle; different bundles vibrated with different amplitudes and frequencies (see Fig. 10); and the frequency of oscillation coincided well with the frequency at which each hair cell was most sensitive to driven displacements. A more likely interpretation of these results is that each bundle is undergoing an actively driven narrow-band oscillation in the absence of an external stimulus to the bundle. Indeed the movements are so large and the sensitivity of the transduction mechanism so high, that we would expect to find electrical signs of these spontaneous movements in the membrane potential. Fig. 10 shows simultaneous measurements of displacement and membrane potential for two cells using the same fibre. The two quantities fluctuate almost in unison.

DISCUSSION

Hair bundle stiffness

We have measured the mechanical stiffness of hair cell ciliary bundles in the turtle cochlea for submicroscopic displacements producing known receptor potentials. We estimated that an average force of 0·6 pN was required to deflect the bundle tip by 1 nm, although there was a spread in values from different cells, some of which could arise from variation in the fibre's position up the bundle (see below). We have no evidence that there was much variation in the absolute height of the bundles which for most turtle cochlear hair cells is about 6 μm. Our stiffness values are roughly comparable to those measured in hair cells of the frog saccule with an identical technique (mean = 0·132 pN/nm; Ashmore, 1984), and in cells of the guinea-pig

cochlea (0·72 pN/nm; mean of values for the apical turn, Strelioff & Flock, 1984). For both preparations, the bundle heights are similar to those in the turtle. On the basis of our average stiffness value, the bundle has a rotational stiffness (eqn. (4)) of $2{\cdot}2 \times 10^{-14}$ N . m/rad.

Theoretical estimate of bundle stiffness

In the following calculations, leading to an estimate of the bundle stiffness, it will be assumed that each component stereocilium is strongly coupled to its neighbours and moves by flexing close to its basal end. Recent observations on the elaborate

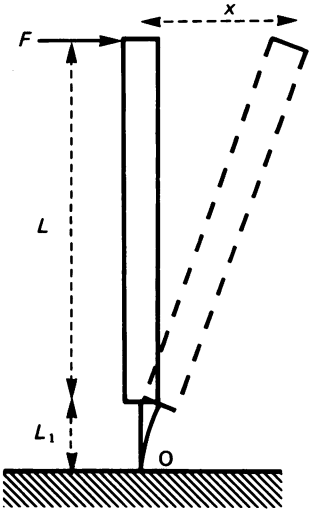

Fig. 11. Schematic representation of a single stereocilium, consisting of a rigid lever attached to a short flexible beam which in turn is anchored to the top of the cell at O. A force, F, delivered to the tip of the cilium produces a deflexion x; x and L_1 are assumed to be small compared to L.

cross-linking of mammalian stereocilia (Pickles, Comis & Osborne, 1984) are consistent with these assumptions. The stereocilium is packed over most of its length with a large number of cross-linked actin filaments, only a small fraction of which (about 25 out of 3000; Tilney, DeRosier & Mulroy, 1980) enter the apical surface of the hair cell and are anchored in the cuticular plate. The simplest model of a cilium therefore consists (see Fig. 11) of a long rigid lever attached to a short flexible beam, clamped at its termination. Experimental evidence supporting this model is: (i) for large displacements that can be visualized, the hair bundle moves as a stiff rod pivoted about its insertion at the top of the cell (Flock *et al.* 1977); (ii) excessive mechanical stimulation causes the stereocilia to be severed at their ankles (Tilney, Saunders, Egelman & DeRosier, 1982), suggesting that the major stress occurs there.

For the model cilium illustrated in Fig. 11, the stiffness, K_1, defined as the force to produce unit displacement at the tip, is given by:

$$K_1 = \frac{2EI}{L_1 L^2}, \tag{6}$$

where L and L_1 are the lengths of the lever and beam respectively, and EI is the beam's flexural rigidity. Since L ($\gg L_1$) is approximately equal to the total ciliary length, this equation indicates that the stiffness will be inversely proportional to the square of this length (see Fig. 4). In a cochlea where the bundles are graded in height, such a relationship implies that, even with constant rotational stiffness, the measured compliance at the tip of the bundle will not be a linear function of the bundle height (Strelioff & Flock, 1984).

Each component cilium of the bundle is assumed to be connected to its neighbours by springs, perpendicular to the axes of the cilia, that can rotate about the points of attachment. Provided these springs are very stiff compared to K_1, the over-all stiffness of a bundle of n_c cilia will be $n_c K_1$. For the turtle cochlea, n_c is about 90 (Miller, 1978). The contribution of the kinocilium will be neglected since its passive stiffness, based on previous measurements of the flexural rigidity of motile cilia (Okuno & Hiramoto, 1979) is estimated to be only a few percent of the measured bundle stiffness.

The bundle stiffness can be deduced if the properties of the beam are specified. From electron microscopic evidence (Tilney *et al.* 1980; Itoh, 1982) the beam is thought to be composed of a small number ($n_a = 25$) of actin filaments which may be cross-linked. For strong cross-linking, the over-all bundle stiffness, K_B, is therefore approximately given by:

$$K_B = \frac{2EIn_c n_a^2}{L_1 L^2}, \tag{7}$$

where EI is now the flexural rigidity of a single F-actin molecule measured as about 4×10^{-26} N.m^2 (mean of values given by Oosawa, 1980). An order of magnitude estimate for the beam length L_1, will be taken as 0·1 μm, and insertion in eqn. (7) of these values along with the other parameters given above yields a K_B of 1·25 pN/nm which is about twice the measured value. If the actin filaments in the ankle of the stereocilium are not cross-linked but can move independently, then K_B is proportional to n_a rather than n_a^2, and the theoretical estimate for K_B is reduced to 0·05 pN/nm. Considering the uncertainties in values for a number of the parameters in eqn. (7), the reasonable agreement between calculated and measured values for stiffness indicates that the simple model for describing passive motion of the bundle is a plausible one. It should be pointed out that in the model, the connexions between cilia were simplified, and it seems likely that a more detailed treatment of bundle motion will need to take into account the mechanical properties of these connexions.

Sensitivity of the transduction mechanism

Best sensitivities reported here for the mechanoelectrical transduction process indicate that the hair cells are capable of generating receptor potentials of a significant fraction of a millivolt for 1 nm deflexion of their ciliary bundles, corresponding to an angular rotation of about 0·01 deg. Our measured mechano-electrical sensitivities are more than an order of magnitude larger than previous estimates derived from manipulation of hair bundles in the frog saccule (20 mV/μm, Hudspeth & Corey, 1977; 7 mV/μm, Ashmore, 1983). Nevertheless, there are several reasons why they may represent only a lower limit to the sensitivities *in vivo*. The maximum peak-to-peak receptor potentials that could be recorded in the isolated

papilla (about 20 mV) are roughly half the amplitude of those seen in recordings from the intact cochlear duct (Crawford & Fettiplace, 1980); this difference may be related to the fact that the ciliary bundles were exposed to perilymph rather than the normal ionic environment of the endolymph. In addition, sensitivities were assayed from the size of the peak of the transient response to a step input, and in a few experiments, we found them to be several times smaller than the sensitivity to a sinusoidal stimulus at the cell's resonant frequency. For a resonant system, the ratio of sensitivities to the two types of stimuli should be approximately equal to the quality factor of tuning (Crawford & Fettiplace, 1981*a*). For the cell illustrated in Fig. 7, which had a step sensitivity of 0·2 mV/nm and a quality factor of 5, the maximum sensitivity to a sinusoidal stimulus at its resonant frequency would have been 1 mV/nm.

We have previously estimated that the turtle basilar membrane would be vibrating with a sinusoidal amplitude of about 0·35 nm peak-to-peak at a sound level equivalent to the animal's behavioural threshold (Crawford & Fettiplace, 1983). It therefore seems reasonable to suppose that at this threshold the hair cells could produce a receptor potential of at least several hundred microvolts.

Passive or active mechanical resonance?

Ciliary bundles execute a damped oscillatory motion when subject to a force step. We can consider whether this property might arise from a passive mechanical resonance of the ciliary apparatus by using the equation of motion,

$$I\ddot{\theta} + R_r\dot{\theta} + K_r\theta = T, \tag{8}$$

where θ is the angular displacement of the bundle, T is the applied torque, K_r is the rotational stiffness of the bundle, R_r the rotational resistance, and I the moment of inertia of the bundle. The passive resonant frequency is given by $(K_r/I)^{\frac{1}{2}}$. The mean value of K_r from our measurements is $2{\cdot}2 \times 10^{-14}$ N . m/rad. The moment of inertia of a single stereocilium rotating around its base is given by

$$I = \frac{\rho\pi r^2 l^3}{3}, \tag{9}$$

where r, the radius, is about 0·1 μm; l, the length, has an *average* value of about 4 μm; and ρ, the density, is likely to be close to that of water (10^3 kg/m^3). These values give a moment of inertia for 100 such stereocilia of $2{\cdot}3 \times 10^{-25}$ kg . m^2. The precise shape of the ciliary bundle is not very critical in determining I; assuming the bundle to be a solid cone of height 6 μm and radius 3 μm gives a moment of inertia of $2{\cdot}0 \times 10^{-25}$ kg . m^2. On this basis, the expected resonant frequency of the bundle would be around 50 kHz yet our measurements show resonant frequencies as low as 30 Hz; to achieve these low frequencies, the ciliary bundles would have to have effective moments of inertia about a million times larger than any simple physical consideration allows.

This line of reasoning taken together with the mechanical effects of current injection, argues that the oscillations of the bundle require an active contribution from the hair cell, as would arise if there existed within the cell an intrinsic force generator. The simplest explanation might be that the motion is due to volume changes consequent on the influx and accumulation of ions within the cell. It can be

shown, however, that the resulting changes in linear cellular dimensions are likely to be insignificant unless the ions are restricted to a small compartment such as the stereociliary shafts. Alternative explanations for the force generator may depend on the hair cells containing a contractile apparatus. For example, myosin has been demonstrated to occur in mammalian cochlear hair cells (Macartney, Comis & Pickles, 1980; Drenckhahn, Kellner, Mannherz, Groschel-Stewart, Kendrick-Jones & Scholey, 1982) and all other types of hair cell, including those in the turtle cochlea, possess a kinocilium, which has the internal structure of a motile cilium.

An estimate of the strength of the force generator can be obtained if it is assumed that it acts at the top of the ciliary bundle (as would be the case for the kinocilium) causing a 10 nm displacement of a bundle of height 6 μm and stiffness 0·6 pN/nm. The force is thus 6×10^{-12} N, comparable to that developed by a single cross-bridge in skeletal muscle, and the corresponding torque about the base of the bundle $3{\cdot}6 \times 10^{-17}$ N . m. The inferred torque is about an order of magnitude smaller than might be expected from a single motile cilium (Yoneda, 1960).

Motion of the ciliary bundle will be determined by the sum of extrinsic forces and the intrinsic force generated by the hair cell. Therefore, if the force generator is controlled by the cell's membrane potential, it will become part of a feed-back system in which the input to the mechanoelectrical transduction mechanism is regulated by the output, the receptor potential (Weiss, 1982). Since all of our measurements were made under closed-loop conditions, i.e. conditions in which the feed-back loop would be operational, it is difficult at this stage to separate out the contributions of the various processes, and the task is complicated by the existence of voltage-sensitive conductances in the hair cell membrane (Lewis & Hudspeth, 1983). A further limitation is that we are unsure that the displacement at the tip of the bundle reflects the total component of motion as seen by the transduction mechanism. For example, if the active process involved a force perpendicular to the cuticular plate, as has been observed by Brownell (1984) in solitary mammalian outer hair cells, only a small fraction of this would be registered by our detection system. Nevertheless, we have measured oscillations up to 20 nm in amplitude that are certainly large enough to excite the transduction mechanism, and their effect would be most prominent for small imposed displacements of the bundle of a few nanometres. At these low levels of stimulation, the feed-back might serve to enhance the cell's sensitivity in the frequency band around its resonant frequency.

We are grateful to Drs J. G. Robson and J. J. Art for many helpful discussions during the course of this work and for critically reading the manuscript. The work was supported by a grant from the Medical Research Council and a Howe Senior Research Fellowship of the Royal Society to R. F.

REFERENCES

ASHMORE, J. F. (1983). Frequency tuning in a frog vestibular organ. *Nature* **304**, 536–538.

ASHMORE, J. F. (1984). The stiffness of the sensory hair bundle of frog saccular hair cells. *Journal of Physiology* **350**, 20*P*.

BIALEK, W. (1983). Thermal and quantum noise in the inner ear. In *Mechanics of Hearing*, ed. DE BOER, E. & VIERGEVER, M. A., pp. 185–192. Delft: Delft University Press.

BROWNELL, W. E. (1984). Microscopic observation of cochlear hair cell motility. *Scanning Electron Microscopy* **III**, 1401–1406.

CASE, J. & CHILVER, A. H. (1971). *Strength of Materials and Structures*. London: Edward Arnold.

COREY, D. P. & HUDSPETH, A. J. (1979). Ionic basis of the receptor potential in a vertebrate hair cell. *Nature* **281**, 675–677.

COREY, D. P. & HUDSPETH, A. J. (1980). Mechanical stimulation and micromanipulation with piezoelectric bimorph elements. *Journal of Neuroscience Methods* **3**, 183–202.

COREY, D. P. & HUDSPETH, A. J. (1983). Analysis of the microphonic potential of the Bullfrog's sacculus. *Journal of Neuroscience* **3**, 942–961.

CRAWFORD, A. C. & FETTIPLACE, R. (1980). The frequency selectivity of auditory nerve fibres and hair cells in the cochlea of the turtle. *Journal of Physiology* **306**, 79–125.

CRAWFORD, A. C. & FETTIPLACE, R. (1981*a*). An electrical tuning mechanism in turtle cochlear hair cells. *Journal of Physiology* **312**, 377–412.

CRAWFORD, A. C. & FETTIPLACE, R. (1981*b*). Non-linearities in the responses of turtle hair cells. *Journal of Physiology* **315**, 317–338.

CRAWFORD, A. C. & FETTIPLACE, R. (1983). Auditory nerve responses to imposed displacements of the turtle basilar membrane. *Hearing Research* **12**, 199–208.

DRENCKHAHN, D., KELLNER, J., MANNHERZ, H. G., GROSCHEL-STEWART, U., KENDRICK-JONES, J. & SCHOLEY, J. (1982). Absence of myosin-like immuno-reactivity in stereocilia of cochlear hair cells. *Nature* **300**, 531–532.

FLOCK, A., FLOCK, B. & MURRAY, E. (1977). Studies on the sensory hairs of receptor cells in the inner ear. *Acta oto-laryngologica* **83**, 85–91.

GULD, C. (1974). Microelectrodes and input amplifiers. In *IEE Medical Electronics Monographs 7–12*, ed. HILL, D. W. & WATSON, B. W., pp. 1–26. Stevenage: Peter Peregrinus.

HUDSPETH, A. J. & COREY, D. P. (1977). Sensitivity, polarity, and conductance change in the response of vertebrate hair cells to controlled mechanical stimuli. *Proceedings of the National Academy of Sciences of the U.S.A.* **74**, 2407–2411.

ITOH, M. (1982). Preservation and visualization of actin-containing filaments in the apical zone of cochlear sensory cells. *Hearing Research* **6**, 277–289.

KAYE, G. W. C. & LABY, T. H. (1975). *Tables of Physical and Chemical Constants*. London: Longmans.

KEMP, D. T. (1979). Evidence of mechanical non-linearity and frequency selective wave amplification in the cochlea. *Archives of Otorhinolaryngology* **224**, 37–45.

KHANNA, S. M. & LEONARD, D. G. B. (1982). Basilar membrane tuning in the cat cochlea. *Science* **215**, 305–306.

KIM, D. O., NEELY, S. T., MOLNAR, C. E. & MATTHEWS, J. W. (1980). An active cochlear model with negative damping in the partition: comparison with Rhode's ante- and post-mortem observations. In *Psychophysical, Physiological and Behavioural Studies in Hearing*, ed. VAN DEN BRINK, G. & BILSEN, F. A., pp. 7–14. Delft: Delft University Press.

LANDAU, L. & LIFSHITZ, E. M. (1969). *Statistical Physics*, pp. 343–400. Oxford: Pergamon.

LEWIS, R. S. & HUDSPETH, A. J. (1983). Voltage and ion dependent conductances in solitary vertebrate hair cells. *Nature* **304**, 538–541.

LOWRY, O. H. & PASSONNEAU, J. V. (1972). *A Flexible System of Enzymatic Analysis*, p. 247. London: Academic Press.

MACARTNEY, J. C., COMIS, S. D. & PICKLES, J. O. (1980). Is myosin in the cochlea a basis for active motility? *Nature* **288**, 491–492.

MILLER, M. R. (1978). Scanning electron microscope studies of the papilla basilaris of some turtles and snakes. *American Journal of Anatomy* **151**, 409–436.

MOUNTAIN, D. C., HUBBARD, A. E. & MCMULLEN, T. A. (1983). Electromechanical processes in the cochlea. In *Mechanics of Hearing*, ed. DE BOER, E. & VIERGEVER, M. A., pp. 119–126. Delft: Delft University Press.

OKUNO, M. & HIRAMOTO, Y. (1979). Direct measurements of the stiffness of echinoderm sperm flagella. *Journal of Experimental Biology* **79**, 235–243.

OOSAWA, F. (1980). The flexibility of F-Actin. *Biophysical Chemistry* **11**, 443–446.

PICKLES, J. O., COMIS, S. D. & OSBORNE, M. P. (1984). Cross-links between stereocilia in the guinea-pig organ of Corti, and their possible relation to sensory transduction. *Hearing Research* **15**, 103–112.

RHODE, W. S. (1978). Some observations on cochlear mechanics. *Journal of the Acoustical Society of America* **64**, 158–176.

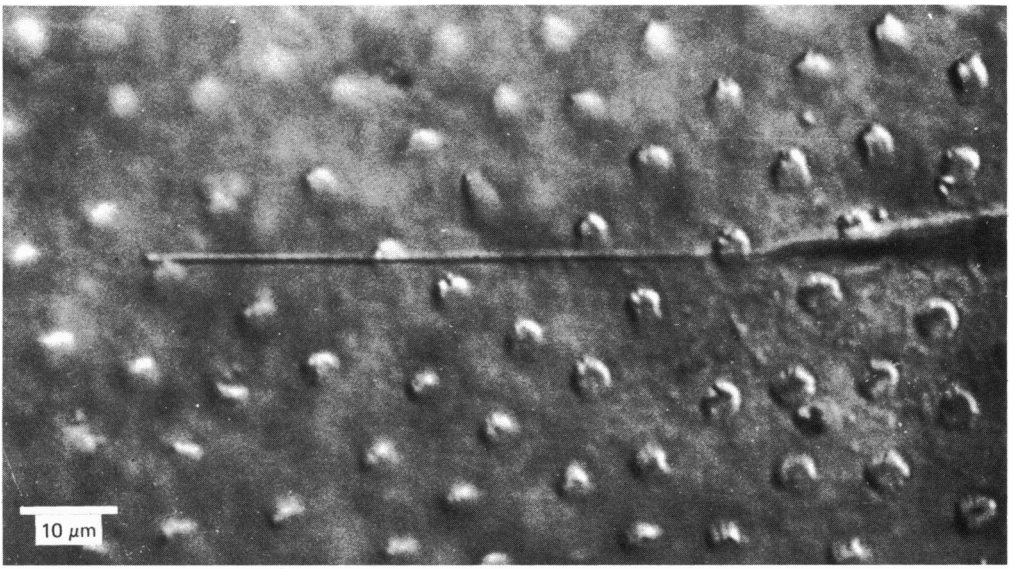
10 μm

SELLICK, P. M., PATUZZI, R. & JOHNSTONE, B. M. (1982). Measurement of basilar membrane motion in the guinea pig using the Mossbauer technique. *Journal of the Acoustical Society of America* **72**, 131–141.

SHOTWELL, S. L., JACOBS, R. & HUDSPETH, A. J. (1981). Directional sensitivity of individual vertebrate hair cells to controlled deflection of their hair bundles. *Annals of the New York Academy of Sciences* **374**, 1–10.

STRELIOFF, D. & FLOCK, Å. (1984). Stiffness of sensory-cell hair bundles in the isolated guinea pig cochlea. *Hearing Research* **15**, 19–28.

TILNEY, L. G., DEROSIER, D. J. & MULROY, M. J. (1980). The organization of actin filaments in the stereocilia of cochlear hair cells. *Journal of Cell Biology* **86**, 244–259.

TILNEY, L. G., SAUNDERS, J. C., EGELMAN, E. & DEROSIER, D. J. (1982). Changes in the organization of actin filaments in the stereocilia of noise-damaged lizard cochleae. *Hearing Research* **7**, 181–197.

WEISS, T. F. (1982). Bidirectional transduction in vertebrate hair cells: A mechanism for coupling mechanical and electrical processes. *Hearing Research* **7**, 353–360.

YONEDA, M. (1960). Force exerted by a single cilium of *Mytilus edulis*. *Journal of Experimental Biology* **37**, 461–468.

EXPLANATION OF PLATE

Photomicrograph of the endolymphatic surface of a turtle basilar papilla, viewed with Nomarski optics to demonstrate the hair cell ciliary bundles. A glass fibre for delivering mechanical stimuli is attached to the kinocilium on the abneural side of one bundle. Kinocilia are visible on several other bundles. The direction of the neural limb is towards the bottom of the plate. Scale bar 10 μm.